Ultramicroscopy 47 (1992) 231–240
North-Holland

ultramicroscopy

Electron holography
II. First steps of high resolution electron holography into materials science

Hannes Lichte, Edgar Völkl
Institut für Angewandte Physik, Universität Tübingen, W-7400 Tübingen, Germany

and

Kurt Scheerschmidt
Max Planck Institut für Mikrostrukturphysik, O-4050 Halle, Germany

Received 9 August 1991; at Editorial Office 15 May 1992

By means of electron holography, the complex electron wave is transferred from the electron microscope to a computer. Consequently, all desirable wave-optical procedures can be numerically applied in a very flexible way to extract and to analyze quantitatively the amplitude and the phase of the object exit wave.

1. Introduction

The determination of the structure of matter by means of electron microscopy essentially involves two steps: The first one is the interaction of the electron beam with the specimen which, in a highly complicated manner described by means of the dynamical theory of diffraction, gives the electron wave at the object exit face. The second step consists of imaging of this object wave on the final screen at high magnification and resolution and taking an electron micrograph.

For determination of the object structure from the micrograph, the two steps have to be inverted, i.e. the two following problems have to be solved: First, the object wave has to be determined from the image. This is difficult to perform from a conventional electron micrograph since it represents only one quantity, i.e. the intensity of the image wave, whereas the information about the object structure is encoded in two different quantities, namely amplitude and phase of the object wave. Electron image plane off-axis holography [1] using the electron biprism [2] is going to solve this problem in the following way: both amplitude and phase of the image wave are recorded in a hologram which is fed to a computer; thereby wave-optically coupled to the electron microscope, the computer represents an expansion of the microscope, which allows one to take all wave-optical measures in real space and in Fourier space needed for the determination of the (complex) object wave.

Second, the so-called inverse problem has to be solved, i.e. one has to determine the underlying object structure from the given object wave. Since there is not yet a general solution, usually the interpretation of an electron micrograph is helped by comparison with the results of image simulation. This time-consuming "trial-and-error" method, however, needs an amount of a-priori information and assumptions about the object structure to be determined. Unfortunately, holography cannot solve the inverse problem, either.

2. Facilities of holography

The procedures for taking a hologram and for the numerical reconstruction of the complex electron wave are described in detail in the preceding paper [3]. The most essential point is that, after the first steps of reconstruction, the complex Fourier spectrum of the image wave is available in the computer quantitatively by amplitude and phase for subsequent numerical processing. In comparison with the Fourier spectrum found in the back focal plane of the electron microscope there are some differences: the contributions from higher spatial frequencies are damped by the incoherent attenuation functions due to chromatic aberration of the objective lens and the finite beam divergence. Additionally, the Fourier spectrum exclusively represents the pure "zero-energy-loss" information about the object: in the electron microscope, the inelastic interaction with the object at an energy loss ΔE gives rise to a time-dependent phase factor $\exp[i2\pi(\Delta E/h)t]$ of the corresponding electron wave with respect to the reference wave [4]. If ΔE is not much smaller than h/τ, i.e. 10^{-15} eV, the respective contribution to the hologram is smeared out during exposure time τ. Consequently, inelastically scattered electrons are not recorded coherently; they rather contribute to an incoherent background of the hologram.

Otherwise, the Fourier spectrum essentially agrees with the complex electron diffraction pattern found in the back focal plane of the objective lens of the electron microscope. In particular, the phases of the reflections are still falsified according to the wave aberration of the objective lens, e.g. by spherical aberration, astigmatism and defocus. Advantageously, one may use the symmetry properties of the spectrum to estimate an actual crystal tilt of the area recorded in the hologram in the same way an electron diffraction pattern may be used when setting the crystal tilt in the electron microscope; this is not straightforward from a diffractogram of a conventional mi-

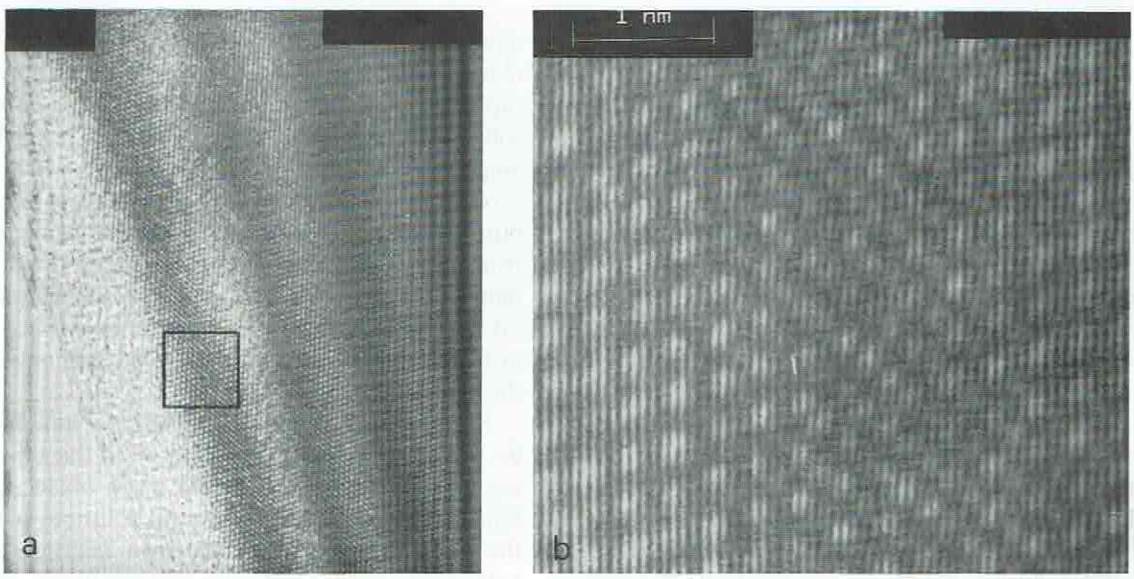

Fig. 1. Hologram of a wedge-shaped Si crystal in (110) orientation. The thickness of the crystal increases from left to right, extinction contour lines run diagonally across the field of view. In the magnified part (b), the interference fringes reveal a moderate phase shift due to the atomic colums at left and at right, whereas strong phase shifts appear in the extinction contour area in the middle.

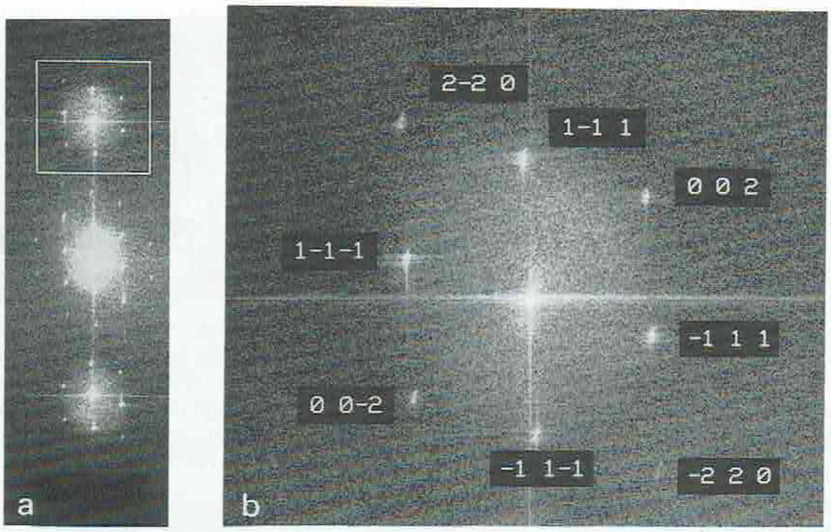

Fig. 2. Fourier spectrum of the hologram (a) and the enframed sideband (b) representing the diffraction pattern of the (110) Si crystal used for reconstruction in the following. The lack of symmetry found in the sideband with respect to the optic axis indicates a slight mistilt from the 110 zone axis. The 220 reflections contribute 0.192 nm spacings to the reconstructed wave.

crograph, which, in principle, is symmetric with respect to the optic axis.

Starting from the reconstructed Fourier spectrum of the image wave, the further imaging process is performed in the computer as if in a perfect "microscope" in that the application of arbitrary phase plates or apertures is not hampered, and amplitudes and phases can be evaluated at every stage. In first place, spherical aberration, astigmatism and defocus are corrected by means of a corresponding phase plate [5]; consequently, the correct phases are available in Fourier space, i.e. there is no phase problem in electron holography. Then, by means of corresponding software, all wave-optical techniques are readily established in a very favourable way both in Fourier space and in real space, and one can easily switch back and forth from Fourier space

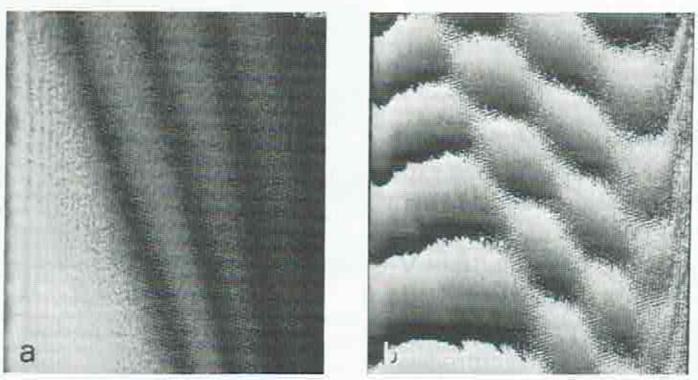

Fig. 3. Amplitude (a) and phase (b) of the image wave reconstructed from the sideband of the Fourier spectrum without taking any correction measures. At the extinction thicknesses the extinction contour lines show up in the amplitude. The lines of equal phases mod 2π display sudden phase jumps at the extinction thicknesses.

to real space. Therefore the methods desirable in electron microscopy can be performed with considerably higher precision and flexibility.

After inverse Fourier transformation of the Fourier spectrum taking into account all reflections, amplitude and phase of the object wave are displayed. Since this can be done over a wide range of defocus, focal series – if they are of any interest at all – can be produced at an arbitrary accuracy of focal steps [6]. Likewise, the distributions of amplitude and phase in real space contributed from single reflections selected beforehand can be determined. By masking off parts of the Fourier spectrum by means of numerically generated apertures of any size and shape for Fourier filtering, e.g. lattice imaging or dark field imaging is easily obtained.

In electron microscopy, the selected-area diffraction is widespread for structure analysis of small object areas. However, this technique is only applicable to areas more than approximately 100 nm wide because smaller apertures are not available; in addition, there arises the problem that, due to the spherical aberration of the objective lens, a very small selected area cannot be associated uniquely to the found diffraction pattern. By holography, a considerable improvement is opened up for the recovery of the complex diffraction pattern from very small object areas only a few nanometers wide. It can be applied to determine the local change in electron diffraction, e.g. due to bending or change in thickness of a crystal.

3. Experimental results

After development of electron holography at atomic dimensions [7], we began to realize experimentally the possible applications sketched above. In the following, some recent results are presented. The holograms were taken at 100 kV by means of a Philips electron microscope EM420 ST with field emission gun, the reconstruction procedures are based on the image-processing software IMAGIC [8].

In fig. 1, a hologram of a perfect, wedge-shaped silicon crystal in (110) orientation is shown. Three

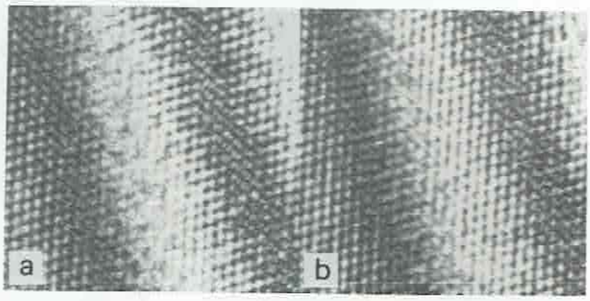

Fig. 4. Amplitude before (a) and after (b) correction of aberrations in the area between the first and second extinction contour line. After correction the weak phase granulation due to the amorphous silicon oxide layer is suppressed, and the lattice fringes are shifted to their approriate position. Note that 0.192 nm spacings are present in both cases.

extinction contour lines are running across the field of view. In the enlarged part one sees that the hologram fringes are slightly curled at the positions of the atomic columns at the very thin edge of the crystal. With increasing thickness, approximately in the middle of the extinction contour line, however, much stronger phase shifts show up, which disappear again on the thicker side. Fig. 2 shows the Fourier spectrum of the crystal, which, by a slight asymmetry, indicates a slight mistilt of the crystal with respect to the selected 110 zone axis. In the reconstructed image wave represented in fig. 3, strong modulations both in amplitude and phase show up at the extinction thicknesses. The effect of correction of aberrations – we found a slight astigmatism, spherical aberration and defocus – can be seen in fig. 4: the lattice fringes from the different reflections are laterally shifted into their (hopefully) appropriate position.

To investigate the effect of the increasing thickness of the crystal on the scattering amplitudes and phases more clearly, prior to the inverse Fourier transformation, masks were applied in Fourier space to screen off everything but one reflection at a time. Such reconstructions have already been reported for the (000) beam by Hanszen [9] from holograms taken at medium resolution. The reconstructions from off-axis reflections, however, can only be performed from high-resolution holograms. The results obtained here for the (000) and the four (111) reflections are shown in fig. 5: in the image waves reconstructed from the single reflections, at the "extinction thicknesses" strong modulations show up in the amplitudes, and sudden phase jumps occur. A closer comparison reveals considerable differences between the amplitudes and phases of the four (111) reflections, respectively, which would not occur at exact excitation of the 110 zone axis; this, again, suggests a small mistilt of

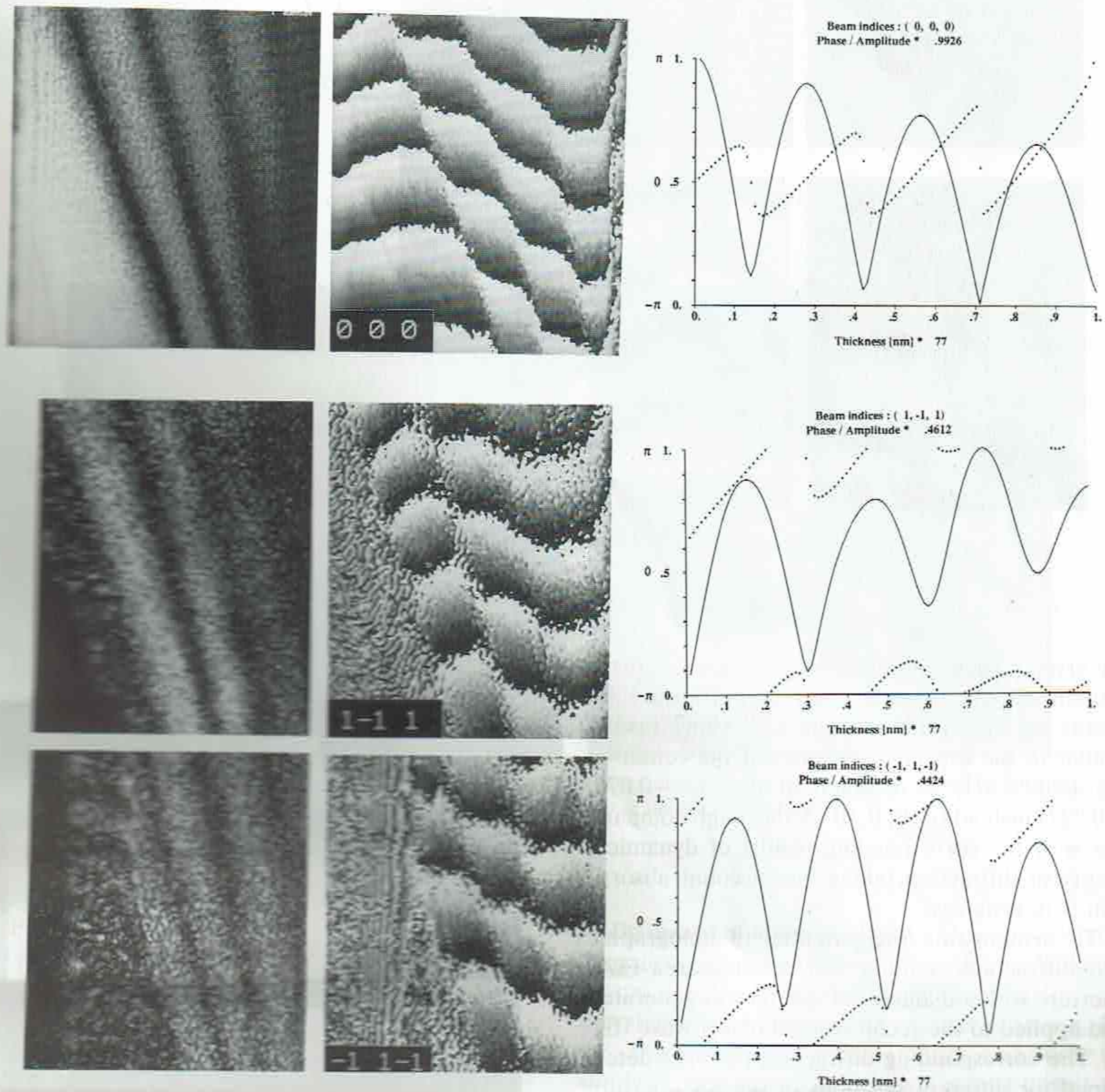

Fig. 5. Image wave reconstructed from single selected reflections of the Fourier spectrum. The amplitudes (left) exhibit the oscillations of the structure amplitudes with increasing thickness of the crystal. The phases (middle) represented by lines of equal phase show sudden phase jumps at the minima of the amplitudes. Due to the mistilt from the 110 zone axis, the {111} reflections behave differently. The corresponding amplitudes and phases of the reflections plotted versus the thickness of the silicon crystal (right) are obtained by a multi-slice calculation using the EMS program; the center of the Laue circle was assumed at (0.075, −0.075, −0.227) (Solid lines = amplitudes, dots = phases).

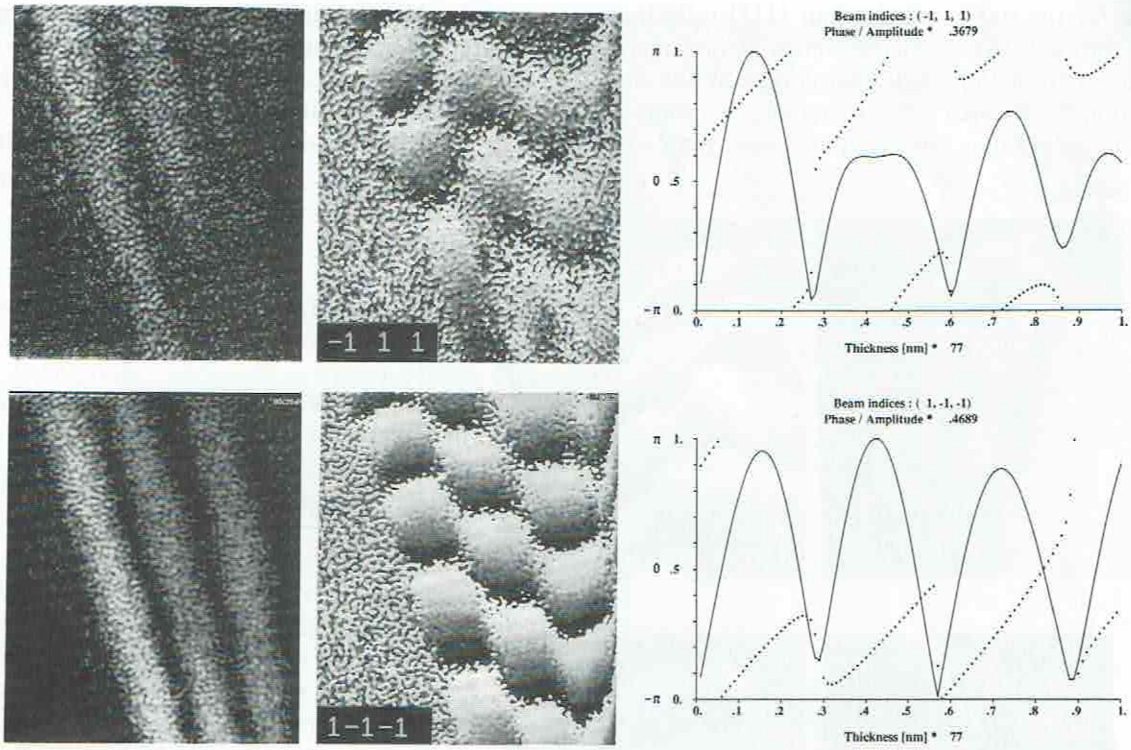

Fig. 5 (continued).

the crystal when the hologram was taken. Corresponding multislice calculations performed by means of the EMS program [10] show results similar to the experimental ones, if the center of the Laue circle is assumed at (0.075, −0.075, −0.227) instead of (0, 0, 0). A thorough comparison with the corresponding results of dynamical theory of diffraction taking into account absorption is in progress.

To demonstrate the potential of holographic nanodiffraction, a numerical selected-area (SA) aperture with a diameter of 2.2 nm was generated and applied to the reconstructed object wave (fig. 6). The corresponding diffraction patterns determined for different positions of the SA aperture show very clearly that the intensities of the different reflections vary differently when the aperture is shifted across the crystal towards larger thickness. This, of course, is to be expected from the dynamical theory.

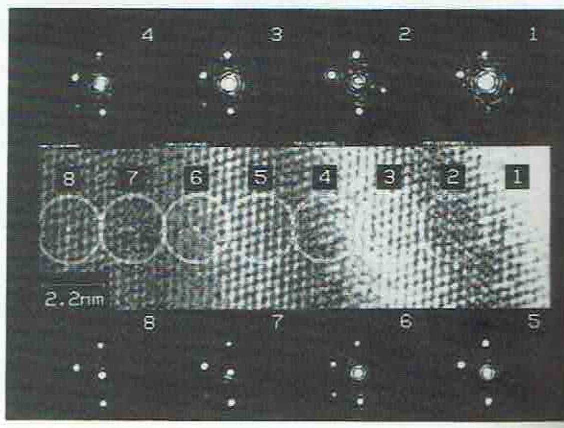

Fig. 6. Numerical nanodiffraction at the Si 110 crystal. A 2.2 nm wide "selected-area" aperture is shifted across the crystal wedge; at the 8 indicated positions the Fourier spectrum is determined. With increasing thickness of the crystal (positions 1–8), the intensity of the different reflections strongly oscillates differently.

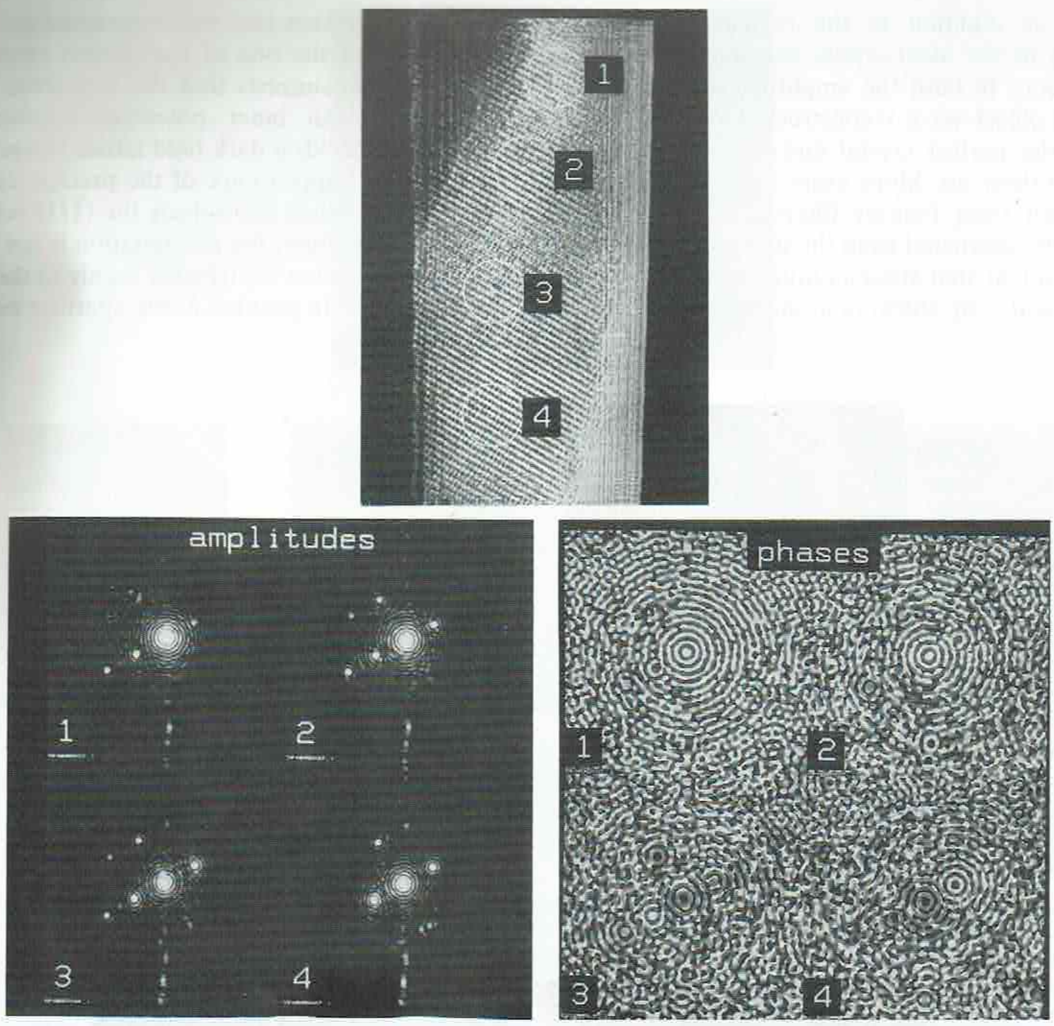

Fig. 7. Nanodiffraction patterns at different areas of a Nb_2O_5 crystal of even thickness reveal a twist of the crystal by the appearing and disappearing reflections. Diameter of the aperture 4.4 nm.

Performing this procedure in the case of a Nb_2O_5 crystal which does not exhibit extinction contour lines, the nanodiffraction pattern changes considerably for the different position of the aperture (fig. 7). Since the change of the diffraction pattern consists mainly of a change of symmetry, it presumably indicates a slight twist of the crystal about the average orientation. Evidently, small local changes in the orientation of a crystal, e.g. due to bending, can readily be determined by this technique.

By means of a non-perfect CeO_2 crystal, which contains a precipitation – presumably – depleted of oxygen, the potential of holography for the investigation of non-perfect crystals is shown. In fig. 5 the sideband of the Fourier transform of the hologram clearly indicates a strong mistilt of the crystal; this information cannot be obtained easily from the autocorrelation in the center, which corresponds to the diffractogram of the respective conventional micrograph. In the sideband, reflections from a "superstructure" are found in addition to the regular ones, which belong to the ideal crystal surrounding the precipitation. In both the amplitude and the phase of the object wave reconstructed with all reflections the perfect crystal and the superstructure clearly show up. More exact information can be obtained from Fourier filtering (fig. 9): In the wave reconstructed from the (000) reflection only, it is evident that the amplitude is more strongly weakened – by absorption, inelastic scattering or strong diffraction into the superstructure reflections – than the one of the perfect crystal; the phase image suggests that the two areas have a different mean inner potential. Applying the aperture 2 yields a dark field lattice image with a very distinct appearance of the precipitation and the crystal. When one selects the $(\bar{1}\bar{1}1)$ reflection for reconstruction, the precipitation is not visible, i.e. this reflection contributes evenly to the whole field of view. In position 4, the aperture evidently

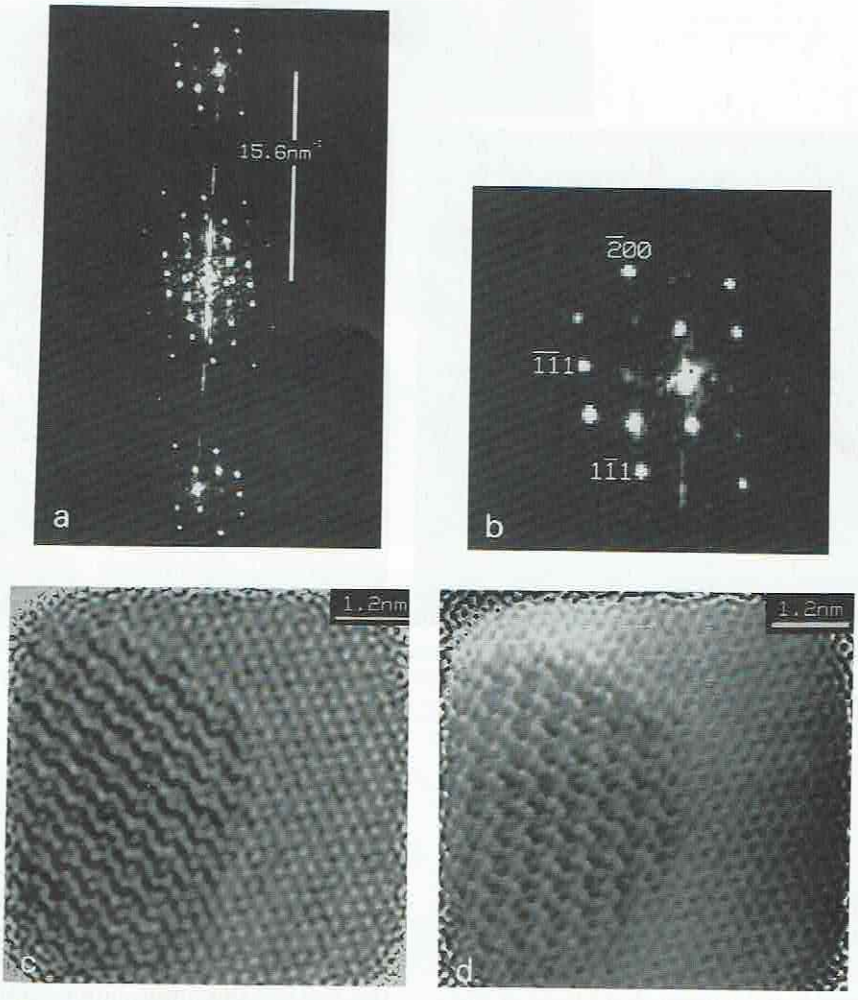

Fig. 8. (a) The sidebands of the Fourier transform of the hologram of a CeO_2 crystal indicate a strong mistilt by the asymmetrical intensity distribution of the reflections. The center band, i.e. the Fourier transform of the image intensity, always reveals point symmetry and nonlinear contributions. (b) In addition to the indexed reflections of the perfect crystal structure, there are several reflections belonging to a superstructure produced by a precipitation. Both amplitude (c) and phase (d) of the reconstructed object wave show a structure of the precipitation which is very different from the perfect crystal.

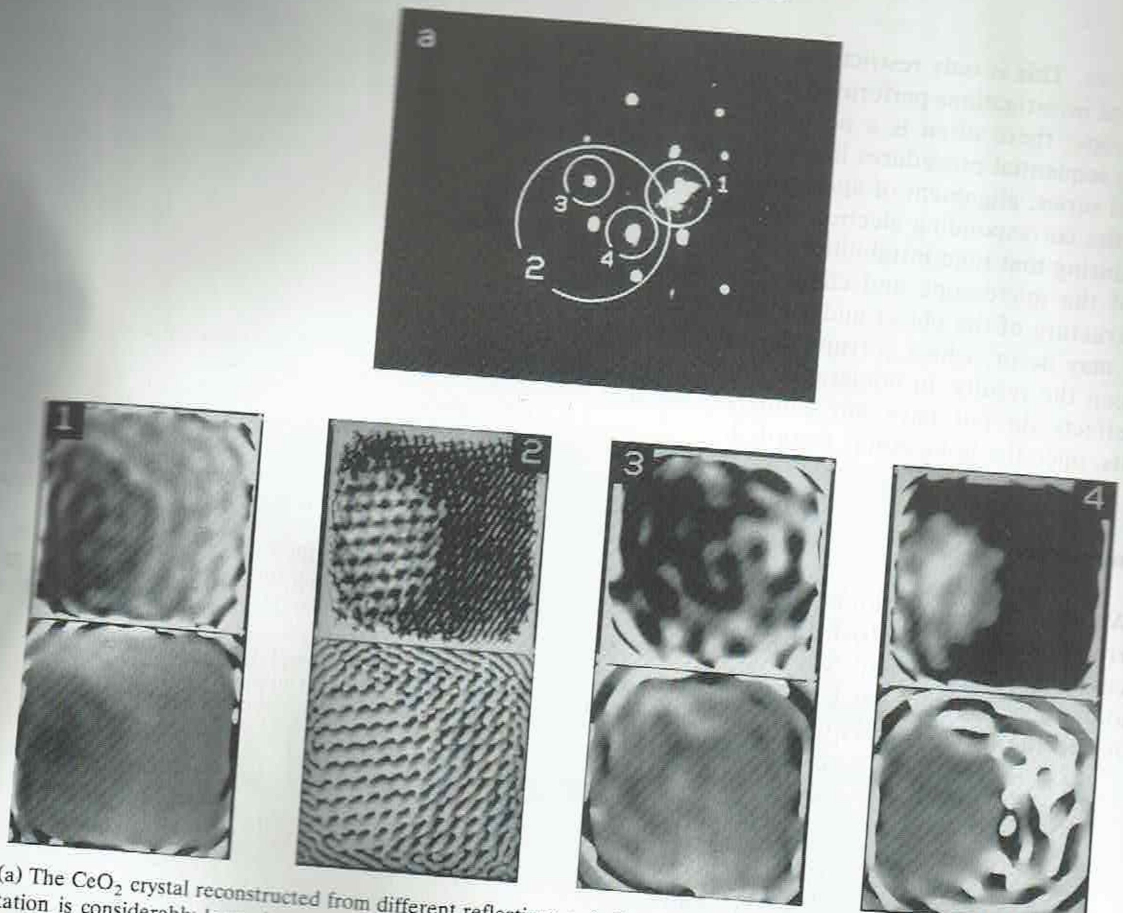

Fig. 9. (a) The CeO_2 crystal reconstructed from different reflections as indicated in the Fourier spectrum. (1) The amplitude in the precipitation is considerably lower because of either higher inelastic scattering or the strong diffraction into the superstructure reflections. The phase modulation by the precipitation is considerably different from the perfect crystal area. (2) Admitting several off-axis reflections to the object wave yields completely different lattice fringe pattern in the precipitation, both in amplitude and phase. (3) In the wave reconstructed from the regular reflection, no differences show up between the precipitate and the perfect crystal. (4) This reflection is a pure superstructure reflection which contributes only to the precipitation, outside of which only noise is found. (Top row = amplitudes, bottom row = phases.)

cuts out a superstructure reflection which arises only from the precipitation.

4. Summary

The presented first applications indicate the high potential of electron holography for materials science at atomic resolution. In addition to the facility for correction of aberrations, the information about the object structure encoded in the object wave is revealed quantitatively by various reconstruction techniques not accessible in conventional electron microscopy. Another essential advantage over conventional electron microscopy is the fact that amplitude and phase information about the object in real space and in Fourier space can be extracted from a single hologram. All results represent the very same object in that they can be related perfectly to each other. This is only restrictedly true for conventional investigations performed in the electron microscope; there often is a need for time-consuming sequential procedures like the production of focal series, alignment of apertures and analysis of the corresponding electron diffraction pattern: during that time instabilities of the parameters of the microscope and changes of position and structure of the object under electron irradiation may occur, which corrupt the relationship between the results. In holography, these annoying effects do not have any influence on the results, once the hologram is recorded.

Acknowledgements

We express our gratitude to Dr. Karl-Heinz Herrmann and Dr. Friedrich Lenz for invaluable discussions. Dr. Eberhard Schweda (Institut für Anorganische Chemie der Universität Tübingen) provided the CeO_2 sample and helped to understand its structure. Qiang Fu helped with his experience in the numerical correction of aberrations. Werner Dreher provided essential software tools for image processing. The financial support from the Körber Stiftung, Volkswagenstiftung und Deutsche Forschungsgemeinschaft is gratefully acknowledged.

References

[1] H. Wahl, Bildebenenholographie mit Elektronen, Thesis, University of Tübingen, 1975.
[2] G. Möllenstedt and H. Düker, Z. Phys. 145 (1956) 377.
[3] H. Lichte, Ultramicroscopy 47 (1992) 223.
[4] G. Möllenstedt and H. Lichte, in: Proc. 9th Int. Congr. on Electron Microscopy, Toronto, 1978, Vol. 1, p. 178.
[5] Q. Fu, H. Lichte and E. Völkl, Phys. Rev. Lett. 67 (1991) 2319.
[6] H. Lichte, Philips Electron Opt. Bull. 130 (1991) 29.
[7] H. Lichte, Adv. Opt. Electron Microsc. 12 (1991) 25.
[8] M. van Heel and W. Keegstra, Ultramicroscopy 7 (1981) 113.
[9] K.-J. Hanssen, J. Phys. D (Appl. Phys.) 19 (1986) 373.
[10] P.A. Stadelmann, Ultramicroscopy 21 (1987) 131.